LEIS FOR THE PREDICTION OF TURBULENT MULTIFLUID FLOWS WITH AND WITHOUT PHASE CHANGE APPLIED TO THERMAL-HYDRAULICS APPLICATIONS

Djamel Lakehal

ASCOMP GmbH
Technoparkstrasse 1, CH-8005 Zurich, Switzerland

Abstract

The paper centers on the use of the so-defined LEIS approach (Large-Eddy & Interface Simulation) for turbulent multifluid flows present in thermal hydraulics applications. Interfacial flows involving deformable, sheared fronts separating immiscible fluids are shown to be within reach of this new approach, featuring direct resolution of turbulence and sheared interface deformations within the Interface Tracking (ITM) framework, such as Level Sets and VOF. In this technique supergrid turbulence and interfacial scales are directly solved whereas the sub-grid (SGS) parts are modelled, at least the turbulence part of it. First results are shown (feasibility), and difficulties and open issues are discussed. The connection between these two particular scales will also be discussed, and potential modelling routes evoked, including combining two-fluid and ITM, local grid refinement, or combing particle tracking and ITM for sub-grid inclusions smaller than the grid size.

1. INTRODUCTION

The computational thermal-hydraulics scene has gone through successive transitions, motivated by new needs and developments. The starting point of the analytical modelling was based on lumped parameter and one-dimensional approaches almost four decades ago, ignoring the shape of the interfaces and neglecting turbulence effects. More refined strategies like the quasi-multidimensional sub-channel models have followed and are still in use for practical safety analysis. The first real transition triggered in the 1980s focused on removing gradually the limitations of 1D modelling by further developing the two-fluid model for 3D turbulent flow problems. This is now the state-of-the-art. The advent of the so-called Interface Tracking Methods (ITM) in the early 90s, which permit to better predict the shape of interfaces while minimising the modelling assumptions for momentum interaction mechanisms, has somewhat shifted the interest, forcing the research towards a new transition. The most recent transition is now underway: it specifically centers on the use of these new simulation techniques (ITM) for practical thermal-hydraulics cases, after it has been validated for canonical two-phase flow problems, including bubble rise, drop splashing or bouncing, stratified air-water flows, and many other examples (Lemonnier *et al.*, 2005). But this latest transition poses interesting challenges to the computational thermal-hydraulics community, and raises some specific questions: how to migrate from averaged two-fluid formulation modeling to more refined interface tracking prediction (or combine them when necessary), and from steady-state Reynolds averaged modelling to unsteady large-scale turbulence simulation. The transition is not a matter of availability of computational power and resources only, but a question of adequacy of code algorithmic (precision), complex meshing, and proper modelling of the underlying flow physics, both in the core and near the interfaces. Some recent developments in this area were reviewed by Yadigaroglu and Lakehal (2005) with emphasis on both single- and multi-phase thermal-hydraulics.

This paper is written in that spirit, centering on a new concept that combines the strength of these ITM methods with the advantage of unsteady, large-scale prediction of turbulence, known as the Large-Eddy Simulation (LES). The outcome of this combination is a better way to capture transients of interfaces and associated turbulence, while minimising modelling (of both: turbulence and interface dynamics). This is the reason why we refer to this approach as LEIS: solving in time as much interface and turbulence scales as possible. We will here limit the mathematical derivations; instead, we will focus on premises, difficulties and required future developments.

2. SCALE SEGREGATION IN MUTLIPHASE FLOW

2.1 Nature and forms

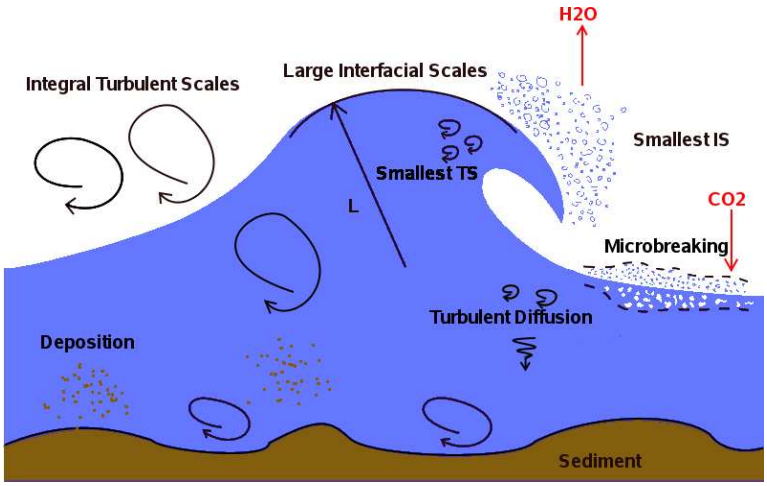

Figure 1: An idealized wave representation.

Multiphase flows appear under various forms depending on the nature of the involved fluids and their rate of presence in the system. A fluid-fluid system may be defined as a ”mixed flow” if the transported phase is rather dilute in the carrier phase, meaning that the fluids do not exert substantial momentum exchange on each other, allowing the transported phase to diffuse into the carrier media by molecular and turbulent effects. In this class of flow the density ratio between the phases is rather small, e.g. snow avalanches, pollutant motion or sediment transport. A fluid-fluid system can be classified as” interpenetrating media” if the characteristics length scales of the transported phase are high enough such that the momentum exchange mechanisms become important. Here the density ratio between the phases is in general large. This category of problems within reach of this technique encompasses, for example, bubbly plumes and hydrocarbon pipe flows, though essentially true for the bubbly and churn flow regimes. In ”interfacial flows” the fluids are separated by a distinct large-scale interface. Stratified pipe flow and sea water waves belong to this category. Distinct (in shape and density) small entities, such as solid particles, liquid droplets and bubbles form generally a ”dispersed flow” system. What differs the mixed flow from the interfacial and/or dispersed flow is the rate of variation in space of the interface topology, defined here as *interfacial scales* (IS), with a spectrum ranging from sea wave amplitude to bubble or droplet diameter. Turbulence is rather specific to each phase separately, although its creation or dissipation is partly due to the way IS interact with each other. But this is another more complicated facet of the problem beyond the scope of work here.

2.2 Scale segregation

The segregation of scales in multiphase flow is needed to pose the development of numerical and modelling techniques on solid grounds. To illustrate this notion, we proceed by analyzing the canonical wave breaking problem depicted in Figure 1. This flow (it could have been a slug-flow in a pipe; apart from the confinement, indeed) involves a hierarchy of length scales. Further, we need to look at the flow as a combination of *turbulence scales* (TS) acting in tandem with the *interfacial scales* defined previously. As to the flow dynamics, the wave develops by the action of pressure and wind-shear by extracting kinetic energy from the mean flow; it ultimately breaks into small scales and dissipates its energy. The whitecap or a micro-breaking layer, where the fluids are hardly distinguishable, forms subsequent to wave plunging across depth. Turbulence is generated in some specific flow portions, i.e. on both sides of the sheared surface, at the sea bottom created by friction, and subsequent to jet plunging. The spectrum of turbulence varies drastically depending on the

imposed wind conditions and sea depth: very large or integral scales are formed on top by the actions of air entrainment with the waves, whereas smaller ones evolve at the crest of the wave, near breaking, and mostly within the whitecap layer. The core liquid is also turbulent, featuring upwelling motions from below. Sea-spray droplets created by wave plunging disperse and deposit in response to the air-side turbulence. The picture is complete; it needs now to be translated in terms of modeling or simulation principles, more specifically: What is a TS and what is an IS; how much of the TS and IS we wish to capture, for what purpose, and what is the adequate modelling framework for the available computing resources/grids.

The wave scenario requires clearly tailored computational methods since it presents various facets in terms of toplogy/interface scales (IS). Sea sprays dynamics should be simulated using a Lagrangian particle tracking method, because the droplets are typically smaller than the grid size, and therefore not explicitly resolvable. The whitecap mixed layer can only be treated using an averaged two-fluid formulation, because the gas phase is heavily mixed with water. Wave deformations can be simulated using ITM's, because the interface is large and clear enough to separate air from water. Sediment transportation can be simulated using the Eulerian field approach, if the density of the suspended material is not appreciably different from the water density. These CMFD techniques were classified by Lakehal (2002). In this paper we are interested in the interfacial turbulent flow regime only.

3. INTERFACIAL TURBULENT FLOWS

3.1 Dealing with interfaces (IS)

Interfacial flows refer to two-phase flow problems involving two or more immiscible fluids separated by sharp interfaces which evolve in time. Typically, when the fluid on one side of the interface is a gas that exerts shear (tangential) stress upon the interface, the latter is referred to as a free surface. Interface tracking/capturing schemes are methods that are able to locate the interface, not by following the interface in a Lagrangian sense (e.g., by following marker points residing on the interface), but by capturing the interface by keeping track, in an Eulerian sense (the grid is fixed), of the evolution of an appropriate field such as a level-set function, a volume-fraction field, a phase-indicator field or colour function. Broadly speaking, there are two computational approaches to solving interfacial flows: front tracking/capturing and interface tracking/capturing methods.

In front tracking, markers are tracked on an interface in a Lagrangian sense as the interface evolves, although the underlying flow field may be solved on a fixed Eulerian grid. The interface tracking variant treats such problems by capturing the interface via an implicit representation. Examples include the Level-Set method (Sussman *et al.*, 1994), in which the interface is considered to be a level surface of a function that is defined over all space, and the VOF method (Hirt and Nichols, 1978), in which the location of the interface is captured by keeping track of the volume fraction of each computational cell in the grid with respect to one of the fluid phases. Be it as it may, the literature has made it such that the level-set approach, front tracking using markers (Unverdi and Tryggvason, 1994), the Second Gradient (Jamet *et al.*, 2001) and VOF methods are referred to as ITM's (Lakehal *et al.*, 2002a).

ITM's are used for the prediction of two-phase flows requiring precise interface identification. Use is made of a single-fluid set of conservation equations with variable material properties and surface tension forces, a concept known as *the single-fluid* formalism (Kataoka, 1986). The idea is attractive – though expensive- since it offers the prospect of a more accurate strategy than the two-fluid formalism, while minimizing modelling assumptions. Large interfacial deformations are within reach of the method, thus dealing with the 'IS' part of the flow picture discussed previously. The open issue here is the relationship between the largest and smallest IS and their dependence with turbulence.

3.2 Dealing with turbulence (TS)

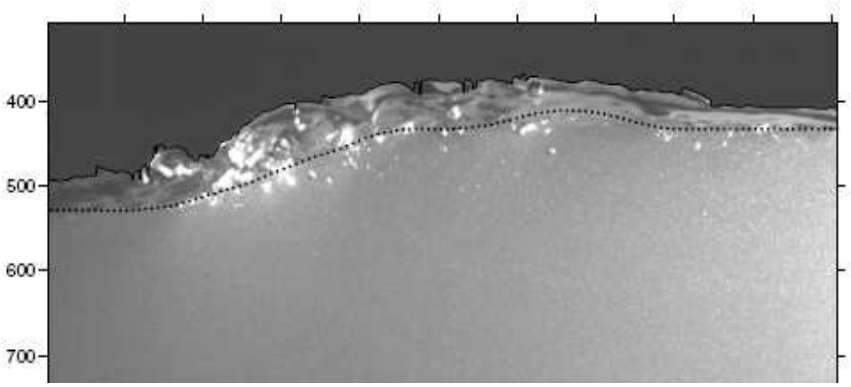

Fig 2: PIV image of hydraulic jump, showing the interfacial boundary layer (Misra et al., 2008).

The turbulence (TS) part of the flow picture refers to the variations of flow scales within each phase, the spectrum of which obeys the well-known 'turbulence cascade', meaning that the largest integral length scales of size L scale with the smallest or Kolomorov length scales (denoted as h) with the Reynolds number raised to some power. This is a well-established theory, valid for high-Re flows in particular. Reynolds averaged Navier-Stokes equations (RANS) are based on averaging the length scales over time, and represent their effects by momentum diffusivity expressed in terms of an augmented viscosity; adding the *so-called* eddy viscosity. Applying this approach in unsteady conditions should predict the most dominant flow modes, like shedding, but still smooth out the sub-scales. The same RANS strategy has been borrowed and applied to two-phase flow problems (mainly bubbly flows) within the two-fluid formulation, with various model adaptations. The limitations of the RANS approach for both single and two-phase flows are now thoroughly quantified.

The picture shown in Figure 2 illustrates best the interaction or co-existence of turbulence and surface deformations in a hydraulic jump (Misra *et al.*, 2008). The solid line depicts the free-surface topology (IS); the dotted line shows the calculated 'mean' actual free surface. The interfacial sublayer is the fluid layer evolving underneath the free surface, delimited by the solid and dotted lines. Turbulence is active in the liquid side as suggested by the illumination technology employed in the experiment, but without providing a clear indication of the size of the structures (TS). The same is true on the upper air side, though not visible in the picture. The interfacial sublayer is substantially sheared and seems to interact with the free surface, which features intermittently high and low curvature areas. To what extent this phenomenon can be affected by underlying turbulence is not clear, however, what matters when it comes to the prediction of this flow is to avoid having to smooth out either surface deformation (IS) and/or turbulence structures (TS).

The combination of LES with one-fluid, IT formulations could lead to the simulation of the large-scale physics in the fluids down to the grid-resolved level (LEIS) of problems similar to the one depicted in Figure 2 above, but understandably not for flows populated by bubbles (for the time being). Recent attempts in our group related to the use of LEIS were successful for turbulent large bubble formation and break-up (Liovic *et al.*, 2003; Liovic and Lakehal, 2007a) and wave breaking (Liovic and Lakehal, 2007b). The idea consists of grid-filtering each phase separately; the resulting sub-grid scale (SGS) stresses are modelled as if they were isolated. Special treatment may be necessary at the interface though, taking advantage of the fact that the lighter phase perceives the interfaces like deformable walls (Fulgosi *et al.*, 2003). In LES, the grid size is related to the smallest resolvable eddy length scale (TS) on each side of the interface. In ITM the smallest IS that can be captured on a given grid is of the order of the grid cell; slightly larger with the Level Set than with VOF for instance. The combination of the two brings a notable difference, that is: besides delivering

the time-dependent interfacial kinematics (and provided the method could achieve sufficient resolution for the boundary layers at the interfaces), the need to model the interfacial exchange terms in the two-fluid phase conservation equations is eliminated. For the time being this is limited to interfacial flows defined above, and will remain not feasible for dispersed gas-liquid flows; the effort needed to track all interfaces and compute accurately the gradients at the interfaces in, say, bubbly flow would have been prohibitive.

3.3 The LEIS alternative

The microscopic, single-fluid equations for incompressible two-fluid flow under isothermal flow conditions known as the one-fluid formulation take the following conventional form (Kataoka, 1989):

$$\frac{\partial \rho}{\partial t} + \mathbf{u}\,\nabla\rho = 0 \qquad (1)$$

$$\frac{\partial \rho \mathbf{u}}{\partial t} + \nabla.\left(\rho \mathbf{u}\,\mathbf{u}\right) = \nabla.\Pi + \rho g + \gamma\,\kappa\,\mathbf{n}\,\delta_s \qquad (2)$$

where $\Pi = -pI + \mu\left(\nabla\mathbf{u} + \nabla^T\mathbf{u}\right)$ is the viscous stress, with **u** standing for the fluid velocity and p for the pressure, ρ is the density, and μ is the viscosity. The third term in the RHS of (2) represents the surface tension force, with **n** standing for the normal vector to the interface, κ for the surface curvature, γ for the surface tension coefficient of the fluid, and δ_s for a smoothed Dirac delta function centred at the interface. Material properties are updated locally based on a phase marker field referred to as C (= 1 in the liquid and = 0 in the gas), denoting a level-set function or a liquid volume-fraction:

$$\rho = \rho\big|_L . C + \rho\big|_G .(1 - C) \qquad (3)$$

Other material properties like viscosity, thermal conductivity and heat capacity are also updated in the same way. To track the interface and update material properties, a topology equation is solved for *C*:

$$\frac{\partial C}{\partial t} + \mathbf{u}\,\nabla C = 0 \qquad (4)$$

In the Level Set technique employed in our code, too, the interface between immiscible fluids is represented by a continuous function ϕ, representing the distance to the interface that is set to zero on the interface, is positive on one side and negative on the other. In the VOF variant, also implemented in our code (Liovic *et al.*, 2006), *C* represents a volume of fluid fraction. ITM techniques refer to the additional algorithms that permit solving (4) without smearing the interface: Level Sets, VOF, etc. Conceptually these methods are in principle capable of capturing the topology of the interfaces, and resolving accurately the interfacial boundary layers, independent from the Reynolds number. If this were the case then these are nothing else than full DNS, since they resolve all TS and all IS motions at the same time. Practically this ultimate goal is rather elusive since the grid necessary to predict the motion of all TS scale with ~ Re^3. Instead, one is forced to solve the flow on grids that scale with $Re^{\mathbf{n}}$, where **n** is clearly smaller than 3, leaving the difference to diffusive-based modelling like in RANS, albeit with a clear separation between resolved and unresolved or sub-grid scales (SGS).

What makes the separation of scales feasible and controllable in the finite-volume/difference concept is the mesh itself, since it reflects the material support for the flow to vary in space and time. We can now re-work the transport equations (1-4) in view of adapting them to this new avenue. In the LES terminology, the flow scales smaller than the grid cell ($\Delta^3 = \delta_x\delta_y\delta_z$) are defined by:

$$f' = \overline{f(x,t)} - f(x,t); \quad \overline{f(x,t)} = \int_D G(x-x':\Delta) f(x',t) dx' \qquad (5)$$

and (unlike in RANS) are such that $\overline{f'} \neq 0$, and where the integral over the entire domain D refers to a convolution product involving a specific space filter G. Rigorously speaking, only spectral CFD codes involve explicit filtering using well-defined filters G (e.g. *Gaussian, top-hat, sharp cut-off*); in finite-volume/differences approaches, however, G is implicitly determined by the grid cell (a sort of *top-hat* filter). This definition applies to the velocity, pressure and temperature fields, but not to material properties, and thus not to the associated phase indicator function C, by virtue of Eq. (3), all the more the hypothesis of dilute phase is not applicable in this context. The LES strategy eliminates thus the statistical averaging of the large scales since it is based on "space filtering". What is the advantage: restrict the modelling to SGS scales which are more homogeneous and uncorrelated with the energetic scales (larger ones), at least for high-Re flows, and thus amenable to more appropriate physical modelling than if we were to deal with the entire turbulence spectrum without distinction.

Be it as it may, the filtered form of the system of equations (1-4) have already been developed (Liovic *et al.*, 2003; Liovic and Lakehal, 2007a,b, Labourasse *et al.*, 2007). The main difference with the filtered single-fluid flow equations is the necessity to consider density and viscosity variations while defining the convolution operation (5). This was first taken into account by Lakehal *et al.* (2002b) in the framework of two-fluid LES by introducing the *so-called* Component-Weighted Volume Averaging (CWVA) using C function; the same could apply to interfacial flows though relying on density rather than on C. More specifically, the filtered system of one-fluid equations read:

$$\frac{\partial \overline{\rho}}{\partial t} + \nabla.\left(\overline{\mathbf{u}}\,\overline{\rho}\right) = 0 \qquad (6)$$

$$\frac{\partial \overline{C}}{\partial t} + \nabla.\left(\tilde{\mathbf{u}}\,\overline{C}\right) = 0 \qquad (7)$$

$$\frac{\partial \overline{\rho}\tilde{\mathbf{u}}}{\partial t} + \nabla.\left(\overline{\rho}\tilde{\mathbf{u}}\tilde{\mathbf{u}}\right) = \nabla.\left[\overline{\Pi} - \tau\right] + \overline{\rho} g + \overline{\gamma \kappa \mathbf{n} \delta_s} + E \qquad (8)$$

where $\tilde{\mathbf{u}}\overline{\rho} \equiv \overline{\rho \mathbf{u}}$ at the interface and $\tilde{\mathbf{u}} \equiv \overline{\mathbf{u}}$ away from it, $\tau \equiv \overline{\rho}(\widetilde{\mathbf{u}\mathbf{u}} - \tilde{\mathbf{u}}\tilde{\mathbf{u}})$ is the SGS stress tensor, E is the sum of the convolution-induced errors that were shown by Liovic and Lakehal (2007a) and Labourasse *et al.*, (2007) to be negligible. Away from the interface the filtered mass conservation equation reduces to a pure divergence of the velocity field: $\nabla.\tilde{\mathbf{u}} = \nabla.\overline{\mathbf{u}} = 0$. The issue concerning the filtered surface tension has also been resolved by the authors cited above: rigorously speaking, the term $\overline{\gamma \kappa \mathbf{n} \delta_s}$ can be written as $\overline{\gamma \kappa \mathbf{n} \delta_s} = \gamma \overline{\kappa}\,\overline{\mathbf{n}}\,\delta_s + \varepsilon^{\kappa}$, where the error term should be contained within the last sum term in (8). This term was indeed found to be negligible compared to the SGS stress tensor by the same authors, both in 2D and 3D. Furthermore, in almost all ITM methods the use of a filter (e.g. 9-cell stencil) for the surface tension is common to avoid divergence of the solution. Filtering the surface tension force has less to do with turbulence, and should therefore not be necessarily linked to the modelling of the SGS stress tensor, at least not in the same manner.

The term requiring modelling in the above equations is the SGS stress tensor alone. Many model variants have been employed so far, and the conclusion is rather clear (Reboux *et al.*, 2006): the most important element to consider in SGS modelling is to accommodate the decay of turbulence near-interface boundary layers very much the same way as in wall flows. This can be achieved by explicit eddy viscosity damping, with the Dynamic approach of Germano *et al.* (1991), or by the use of the Variational Multiscale Model (VMS) of Hughes *et al.* (2001). In VMS the effect of the unresolved sub-grid scales is restricted to the *small-large* scales, the portion of the turbulence spectrum upper-

bounded by the SGS cut-off and a lower-bounded cut-off twice as large as the first one. The MILES approach (Monotonically Integrated LES) of Fuerby and Grienstein (1990) that leaves the SGS to the numerical truncation errors can also be used for mild-Re flows, within the finite volume approach.

The SGS modelling within the eddy-viscosity framework makes τ_{ij} proportional to the strain rate S_{ij}:

$$\tau_{ij} = -2\nu_t S_{ij} + \delta_{ij}\tau_{kk}/3; \quad \nu_t = f_{\mu-\text{int}}(Cs\Delta)^2\sqrt{2\bar{S}_{ij}\bar{S}_{ij}} \qquad (9)$$

Here the length scale is based on the cell size, and the value of the model coefficient C_S is set equal to 0.1 in the core flow. In the presence of shear – either near the wall or in the vicinity of deformable surfaces where the viscous sublayer is well resolved – eddy viscosity models generally need to incorporate a damping function $f_{\mu\text{-int}}$ in order to accommodate the near-wall/interface limiting behaviour in low-Re number flow conditions. Similar 'corrections' need to be introduced when eddy viscosity models are employed for interfacial two-phase flows, where the lighter phase perceives the surface like a rigid wall (Fulgosi *et al.*, 2003). A systematic LES study of the flow investigated by Fulgosi *et al.* (2003) using DNS performed by Lakehal *et al.* (2005) has shown that without such modification the Smagorinsky model alone becomes excessively dissipative, just as it tends to be for wall-bounded flows. For low to moderate interface deformations the DNS database of Fulgosi et al. (2003) provided an exponential dependence of f_μ^{int} on the distance to the interface for the gas side:

$$f_\mu^{\text{int}} = 1 - \exp(a_0 y_{\text{int}}^+ + a_1 y_{\text{int}}^{+\,2} + a_2 y_{\text{int}}^{+\,3}) \qquad (10)$$

where a_0, a_1 and a_2 are model coefficients, and $y_{\text{int}}^+ = \Phi u_{\text{int}}/\nu$ is the so-called "interface turbulence unit" length scale, defined based on u_{int}, the interfacial shear velocity, and Φ, the distance to the interface (level set function or reconstructed distance to the interface from raw VOF data). In a companion paper (Liovic and Lakehal, 2007b), the authors have introduced and validated the algorithm for extracting the ingredients necessary for estimating this length scale from the flow field – namely the air-side interfacial shear/friction velocity and the reconstructed distance function. The SGS model (9) modified with (10) has been validated by Liovic and Lakehal (2007b) for a Taylor-Couette flow and for the stratified counter-current air-water flow of Fulgosi *et al.* (2003). Actually, a similar near-interface damping is required on the liquid side, too, but this is discussed in a future contribution of the authors.

4. THE NUMERICAL APPROACH

4.1 TransAT© Multiphase Flow Software

The CMFD code TransAT© developed at ASCOMP is a multi-physics, finite-volume code based on solving multi-fluid Navier-Stokes equations. The code uses structured meshes, though allowing for multiple blocks to be set together. MPI parallel based algorithm is used in connection with multi-blocking. The grid arrangement is collocated and can thus handle more easily curvilinear skewed grids. The solver is pressure based (Projection Type), corrected using the Karki-Patankar technique for low-Mach number compressible flows. High-order time marching and convection schemes can be employed; up to third order Monotone schemes in space. Multiphase flows are tackled using interface tracking techniques for both laminar and turbulent flows, where the flow is supposed to evolve as one fluid having variable material properties, which vary according to the colour function as it is advected by the flow, identifying gas flow regions from the liquid phase. Specifically, both the Level-Set and the Volume-of-Fluid methods can be employed to track evolving interfaces.

4.2. The Immersed Surfaces Techniques (IST)

Immersed boundary (IB) techniques have been developed in the late 90s for flows interacting with solid boundary under various formulations. The mostly known formulation for instance employs a mixture of Eulerian and Lagrangian variables, where the solid boundary is represented by discrete Lagrangian markers embedding in and exerting forces to the Eulerian fluid domain. The interactions between the markers and the fluid variables are linked by a simple discretized delta function. IB methods are all based on direct momentum forcing (penalty approach) on the Eulerian grid. The forcing should be performed such as it ensures the satisfaction of the no-slip boundary condition on the immersed boundary in the intermediate time step. This forcing procedure involves solving a banded linear system of equations whose unknowns consist of the boundary forces on the Lagrangian markers; thus, the order of the unknowns is 1D lower than the fluid variables.

The Immersed Surfaces Technology (IST) has been developed by ASCOMP GmbH (to the best of our knowledge), although other similar approaches have been developed in parallel. The underpinning idea is inspired from Interface Tracking techniques for two-phase flows (Level Sets), where free surfaces are described by a hyperbolic convection equation advecting the phase color function. In the IST the solid is described as the second 'phase', with its own thermo-mechanical properties. The technique differs substantially from the Immersed Boundaries method of Peskin, in that the jump condition at the solid surface is implicitly accounted for, not via direct momentum forcing (using the penalty approach). It has the major advantage to solve conjugate heat transfer problems, in that conduction inside the body is directly linked to external fluid convection. The solid is first immersed into a cubical grid covered by a Cartesian mesh. The solid is defined by its external boundaries using the solid level set function. Like in fluid-fluid flows, this function represents a distance to the wall surface; is zero at the surface, negative in the fluid and positive in the solid. The treatment of viscous shear at the solid surfaces is handled very much the same way as in all CFD codes.

4.3. The Block-Mesh Refinement (IST)

The BMR technique was developed in the TransAT code to help better solve the boundary layer zone when use is made of the IST technique discussed above. In BMR, more refined sub-blocks are automatically generated around solid surfaces; with dimensions made dependent on the Reynolds number (based on the boundary layer thickness). An unlimited number of sub-blocks of various refinements can be generated, with connectivity between the blocks matching up to 1-to-8 cells. This method can save up to 75% grid cells in 3D, since it prevents clustering grids where unnecessary.

5. VALIDATION

The stratified air-water flow of Fulgosi *et al.* (2003) is the right validation case for SGS modelling, since a complete DNS data base is available for comparison, and because the flow does not feature interface fragmentation that would have complicated the analysis. Here we compare model (9-10) with the DNS data, the under-resolved DNS without SGS modelling. The comparison includes the results of the VMS approach of Hughes *et al.* (2001), in which in contrast to filtering the equations are derived by applying a priori scale separation to the primitive equations; i.e. by projecting the exact solution on a smaller function space. This virtually avoids having to model the unresolved interfacial scales that appear in the filtered single-fluid equations. Numerical experiments in wall bounded flows have shown the VMS approach to lead to the definition of self-adaptive SGS models, similar to the dynamic strategy based on the Germano identity. This means that it should virtually dispense with near-wall turbulence treatment, which stimulates its extension for interfacial two-phase flows. Specifically, the velocity field is partitioned into coarse-scale and fine-scale components. The dynamic model yields an eddy viscosity with too much activity in the large scales, a difficulty avoided by the VMS approach by restricting the activity to the small-scale portion of the spectrum.

Fulgosi's (2003) flow is well documented in the literature; briefly, it involves turbulent gas and liquid stream flowing in opposite directions in a channel at a shear-Reynolds number of 170 (equivalent to bulk Re = 3400). The sheared interface is allowed to deform in space and time by solving a convection equation for the surface elevation. The DNS solution method uses a pseudo-spectral algorithm, and is referred to as the Boundary-Fitting Method, solving separately the two phases. Details of the comparison are available in Reboux et al. (2006).

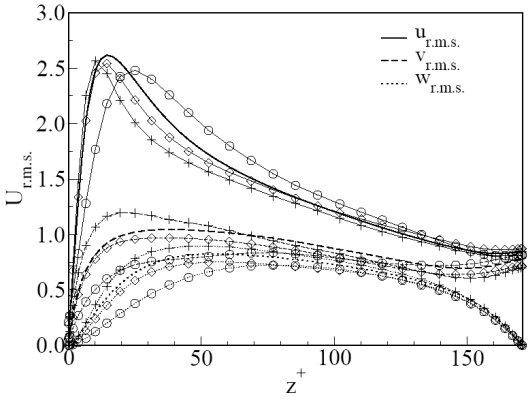

Fig 3a: RMS velocities on the gas side: -- DNS (64^3); 000 Smagorinsky; □□□ (9-10); ++ DNS (32^3).

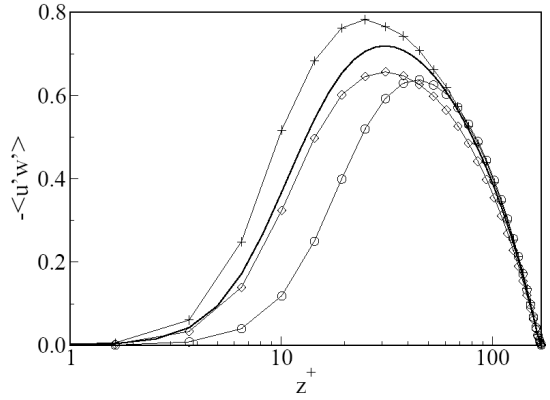

Fig 3b: Shear stress <u'w'> on the gas side: the same nomenclature applies as in left panel.

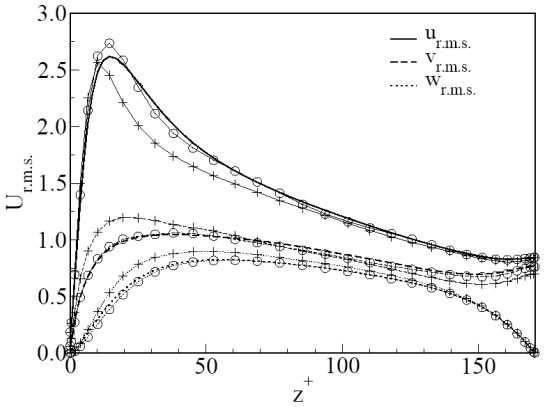

Fig 4a: RMS velocities on the gas side: -- DNS (643); 000 VMS (323); ++ DNS (323).

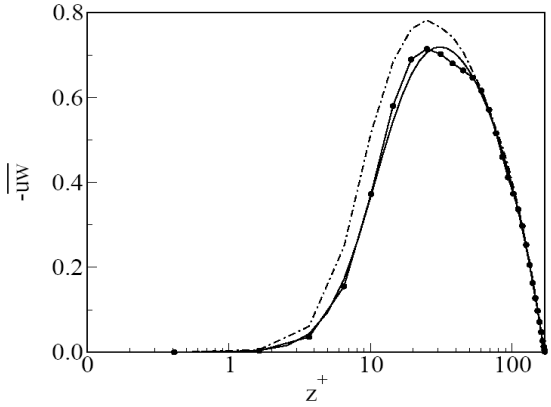

Fig 4b: Shear stress <u'w'> on the gas side: the same nomenclature applies as in left panel.

We first proceed by a comparison between full DNS (64^3), under-resolved DNS (32^3) and selected LES results obtained with the reference and modified Smagorinsky models (9-10); this is discussed in the context of Figs. (3a) and (3b) for the gas phase, where turbulence intensities and shear stress are compared as a function of the non-dimensional distance to the interface; the graphs include the results of the under-resolved DNS (32^3). It is clearly shown that without an SGS approximation the results deviate considerably from DNS. While the fluctuations are underestimated in the streamwise directions, they are grossly overestimated in the spanwise and vertical directions. The SGS model of reference is clearly dissipative, and this can be judged from the shift of the peak in turbulence intensity, which corroborates with the shift in the turbulent shear stress observed in the right panel of the figure. The turbulent shear stress plotted in Fig. (3)b are correctly predicted by model (9-10).

Turning now to the VMS results, overall the quality was better than with model (9-10) but at the expenses of a fine tuning of the model parameters, namely the type and size of the cut-off filter, the

ratio of the two filter widths employed. Figures (4a) and (4b) compare indeed the VMS (32^3) results of the turbulence intensities and shear stress on the gas side. The agreement with the full DNS is perfect; the same is true for all other quantities, on both sides of the interface.

6. PRACTICAL EXAMPLES

6.1 Slug formation in circular pipes

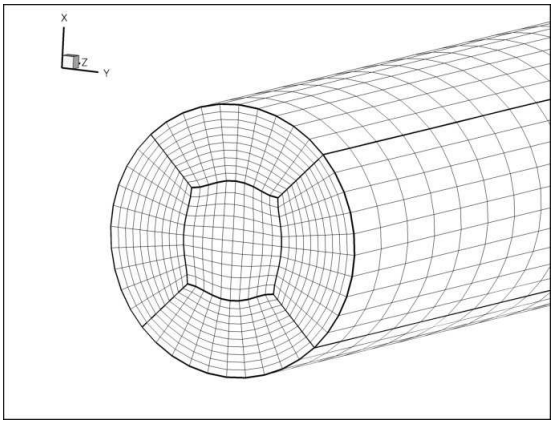

Figure 5: Computational multi-block grid using BFC.

A full 3D computational domain is considered in these simulations. A portion of the grid is shown in Figure 5. The pipe length is 6.3m, and the diameter is 0.14 m. The multi-block grid strategy is used to cover the domain with adjacent sub-domains. Here boundary fitted grids were used rather than the IST. The blocks are distributed between 12 processors for MPI parallel execution. The results presented here were obtained for a grid composed by nearly 360,000 curvilinear cells distributed over 12 blocks. The LEIS approach was employed here, though relying on the Level-Set technique for interface tracking rather than VOF. SGS modelling was achieved using model (9-10). The inflow boundary conditions involve fixing the superficial gas and liquid velocities and the void fraction, as specified in the experiments of Martin et al. (2005). The right-end of the cap was left open now; Neumann boundary conditions for the velocity field were used, in combination with a special scheme for the void fraction to control global and phase-specific volume conservation. Specifically at the inflow, we have set the following values for the turbulent flow conditions: gas superficial velocity = 14m/s; liquid superficial velocity = 0.5m/s; void fraction = 50%. An initial flow disturbance was applied in the entire flow domain, based on the wall shear Reynolds number.

The development of waves in the gas liquid pipe flow is shown for the case of 14m/s inlet gas velocity and 50% void fraction in the next figures. Figure 6 shows successive surface displacements predicted at various successive time steps. A first wave mode is seen to develop under the action of pressure and interfacial shear at about 1.5D from the inflow plane.

The surface of this wave is clearly three-dimensional. Small slope waves are developed further downstream. A second mode is formed in the wake of the first one, which seems to merge further downstream just before slug formation. The slug forms only far downstream at six pipe-diameters from the inflow. The difference with earlier 2D simulations is that the short, low-amplitude waves formed prior to sealing are three-dimensional in nature, distributed non-homogeneously in the spanwise direction over the surface. Other subsidiary modes are subsequently formed, which merge to form new slugs as during the initial stage. Note too that downstream the slug, surface displacements of various slopes and wave lengths are formed, subsequent to the strong interaction of the surface with the gas shear and turbulent structures, as shown in the corresponding section. We also note that the

initial wave mode formed before sealing are laterally inclined, and cannot be considered as sinusoidal waves. The last panel of the figure shows the instability of the wave crest as it seals, leading to strong surface wrinkling, as it has been found in breaking waves by Liovic and Lakehal (2007b).

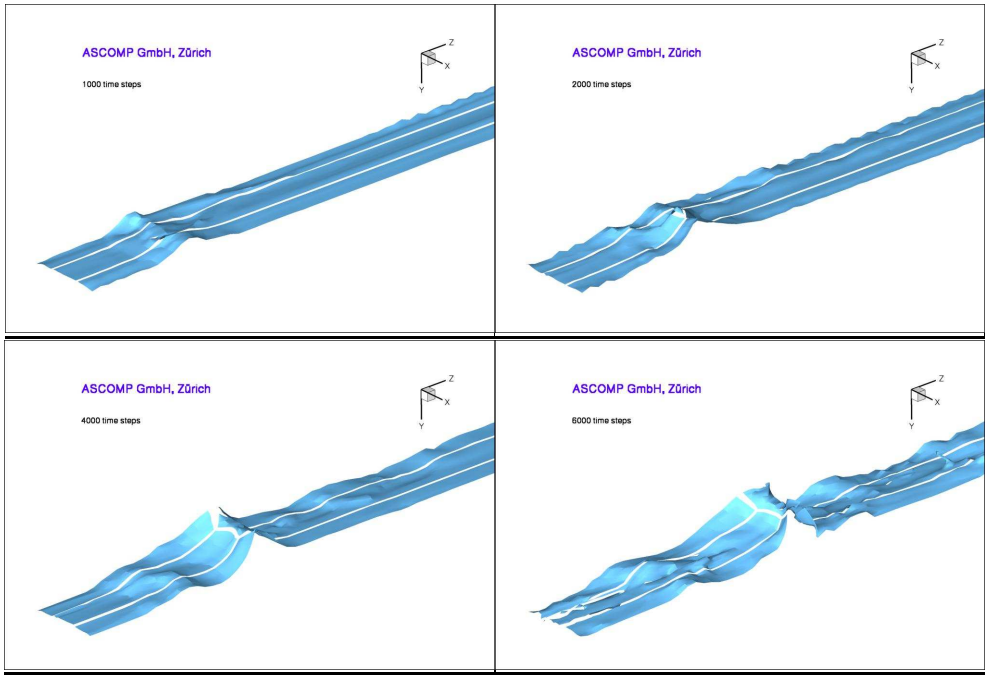

Figure 6: surface displacements at various time instants.

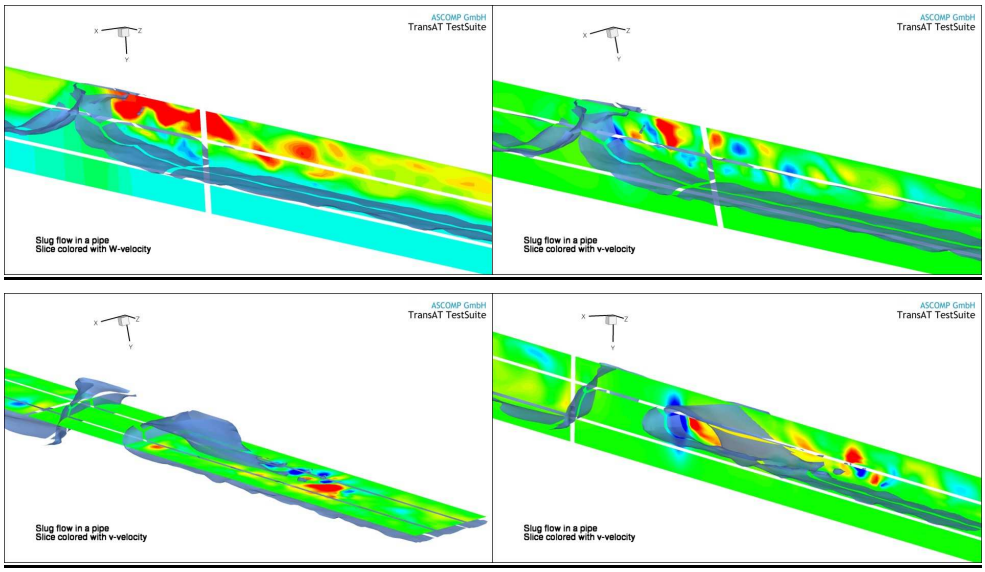

Figure 7: Vortex shedding past the slug coloured by u'_I, highlighting wave breaking after slug sealing

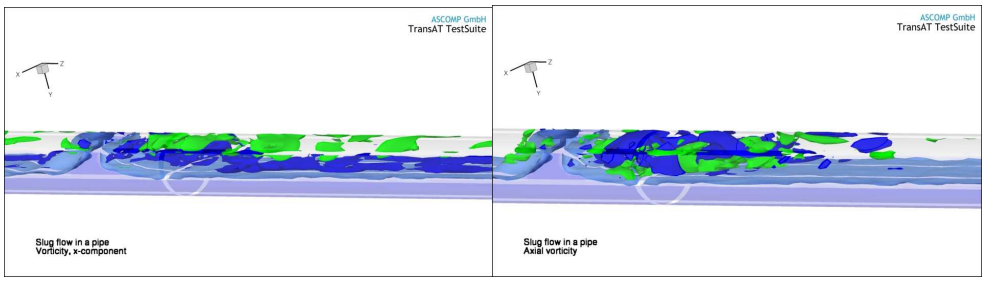

Figure 8: Positive and negative vorticity contours (x and z components)

The subsequent blockage formed by the liquid causes more liquid accumulation with time, and this seems to further isolate the gas slugs. The mechanism repeats itself and successive slugs form along the pipe. Figure 7 shows the iso-contours of the free surface, combined with three velocity contours, each displayed on the 2D central y-z plane. These panels show something unusual, that is the formation of vortex shedding past the slug, immediately after sealing. This observation is corroborated by all three instantaneous velocity- component contours, in particular w'.

The mechanism is similar to what may be expected in flows past fixed blunt bodies; the slug plays somehow the same role, as it travels with a lower velocity than the gas after sealing. The breaking of the free surface after slug sealing is also perfectly illustrated in Figure 7. Again, the panels combine free-surface and velocity iso-contours. The figure shows the vigorous plunging of the breaker after sealing, pretty much similar to what we observe in plunging breakers. The third panel shows in particular the impact of the breaker over the stratified liquid surface, a region characterized by a very high level of turbulence production. Vortex shedding is again visible as in the previous panels, though the breaker seems to have affected the coherence of their motion.

The flow is also shown to be populated by coherent structures, pretty similar to turbulent channel flows. This is illustrated in Figure 8, displaying positive and negative vorticity levels. It seems once more that turbulence is particularly active downstream of the slug, even before the slug breaks. Turbulence production is very high at the impingement of the wave tongue, and should ultimately penetrate underneath the surface. The organisation of these structures as well as turbulence production and transport are similar to those revealed in breaking waves (Liovic & Lakehal, 2007b).

The slug tail and centre speeds are discussed in Figure (9) below, displaying the position of the slug versus time. A linear dependency is revealed, which is in agreement with the measurements of Martin et al. (2005), who obtained an average slug speed of U_s=9.4 m/s, under these conditions. Under these conditions, the slug speed is rather constant, as it has been found in the earlier 2D simulations (results not shown here). In case of the hydrodynamic slugging, the slug velocity can be calculated from gas and liquid flow rates if the void fraction is known, in horizontal lines the mean velocity of the liquid in the body of the slug is approximately equal to the mixture velocity, or can be estimated analytically (Collins et al., 1978) using:

$$U_s = 1.201 U_m + 0.532\sqrt{Dg\left(\rho_l - \rho_g\right)/\rho_l} \qquad (11)$$

where U_m stands for the mixture velocity. The result shown in Figure (9) reveal that our LESI simulation predicts the slug speed (tail and centre) in accord with the theory (11), which gives U_s=9.33 m/s, and experiment of Martin et al. (U_s=9.4 m/s). This is an interesting result for practical applications, which shows that although a coarse grid has been used, the LEIS concept is capable to predict one of the most important flwo feature of pipe flows.

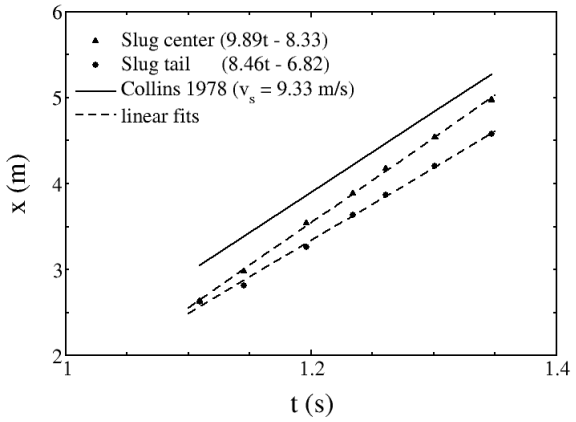

Figure 9: Slug speed (tail and centre): LES vs. Analytical solution

6.2 Fuel bundle analysis

This thermal-hydraulics problem is very challenging from all the aspects. It concerns the simulation of flow characteristics in hydraulically equilibrium two-phase flow in a vertical 2-3 rod bundle sub-channel of Sadatomi et al. (2004). The experiments were carried out using water and air at ambient pressure and temperature as the working fluids and a 2-3 rod bundle channel as the test channel, containing six rods in rectangular array and two-kinds of six sub-channels, simulating a BWR fuel rod bundle (Fig. 10). Flow distribution data and pressure drop along each sub-channel axis were obtained in various single- and two-phase flows under hydraulic equilibrium flow conditions. The dimensions of the experimental setup are as follow: Rod diameter: d = 16 mm; Rod pitch: p = 20 mm; Pitch to diameter ratio: p/d = 1.25; Gap clearances: $S_{11} = S_{12} = S_{22}$ = 4mm; Hydraulic diameter: D_h =14.3 mm; Flow area: A = 194 mm2.

Here the IST method explained previously has been applied to avoid having to deal with BFC grids for each tube, like in Fig. 5. Tube surfaces from a CAD file are embedded within a Cartesian equidistant grid, which reduces drastically grid-skewness induced errors. The length of the computational domain was reduced to L = 120 mm and the tube length to L_t = 20 mm. The width of the domain was set to W = 30 mm. The grid consists of 65x65x130 cells. Inflow and outflow boundary conditions were set at the bottom and top parts of the channel. The simulations were executed on a parallel Quad-core 8-Processor Linux PC cluster; 24H clock time were necessary for the flow to fully develop. Note here that no attempt was made to reach real statistical conditions for averaging; the exercise is meant first to show the potential of ITM's (Level Sets here) to track complex topology changes in a non-isothermal two-phase flow, with conjugate heat transfer.

In the prediction of thermal-hydraulic behaviour of a coolant in a BWR fuel rod bundle, it is necessary to evaluate accurately fluid transfer between sub-channels. The fluid transfer in the two-phase system consists of three independent components; void drift, diversion cross-flow and turbulent mixing. In contrast to the previous example, here, too, the flow is multi-scale, including fluid flow and conjugate heat transfer. Phase change was not activated here to mimic the experiment.

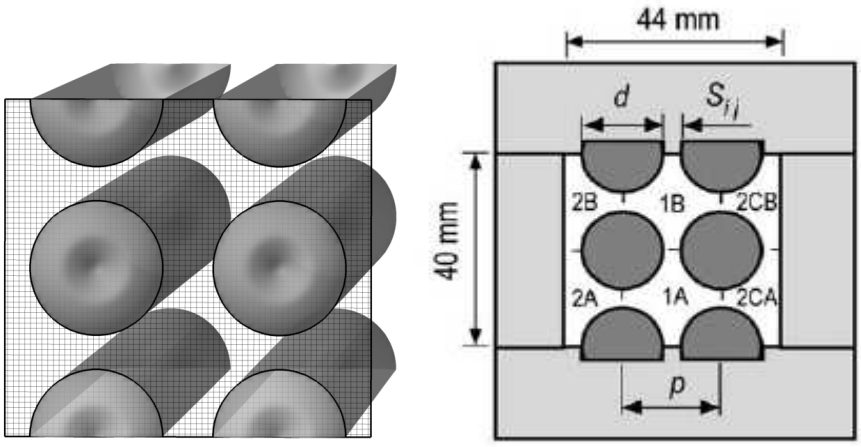

Figure 10: IST grid and cross-sectional geometry and dimensions of the test channel.

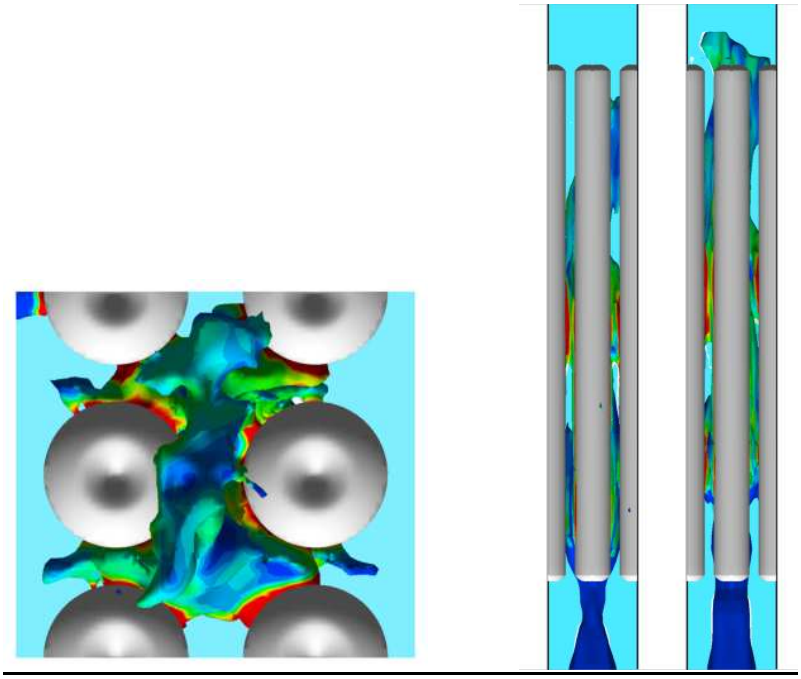

Figure 11: 3D and side view tubes showing tube temperature and gas topology: Turbulent flow (Re=16.000).

As to turbulence, we have again used the MILES approach of Fuerby and Grienstein (1990) because the bulk Reynolds number is not very high (Re = 16.000), where the diffusive effect of the advection scheme plays the same role as an explicit SGS model for LES. We are now testing a scale separation approach, in which the diffusive effect of the turbulent sub-scales are treated with the numerical truncation errors, while larger scales (not fixed by the grid size) are directly simulated (a sort of V-LES; or Very Large-Eddy Simulation – V-LES). The concept of V-LES (Speziale, 1997) means that the length scale used for the SGS modelling is not necessarilly dictated by the size of the cell is in the pure LES. The approach may be viewed as an alternative to both LES and unsteady RANS; it is somewhat similar to the SAS strategy.

Two cases were simulated: a laminar flow with water inflow velocity U_L = 0.1 m/s (results of which are not discussed here), and a weak turbulent case with water inflow velocity U_L = 1 m/s; in both case the inflow void fraction is 50%.

Figure 11 (left) depicts the cross-channel section showing the heat contours developing between the tubes together with the gas-liquid interface, for the turbulent case. The right panels show the side view, at two instants. The temperature distribution inside the tube is not shown. Because the central tubes are exposed to a higher surface exchange area with the gas phase, these are subject to a higher heat removal rate. The interface (coloured by temperature) is shown to be highly deformed by the flow, causing a random heat transfer from the tubes. The oscillation of the two-phase flow along the tube is well illustrated in the right panel, showing in particular that the heat removal rate from the tubes is larger in the central part of the tubes. Again, this exercise is the first step towards a full description of sub-channel analysis using CMFD, with a minimum number of models. There is no pretention here that this simulation has captured all the relevant phenomena, rather, the attempts paves the way for more detailed simulation, requiring probably a more refined grid and more CPU time.

6.3 Emergency Core Cooling (ECC): the COSI experiment

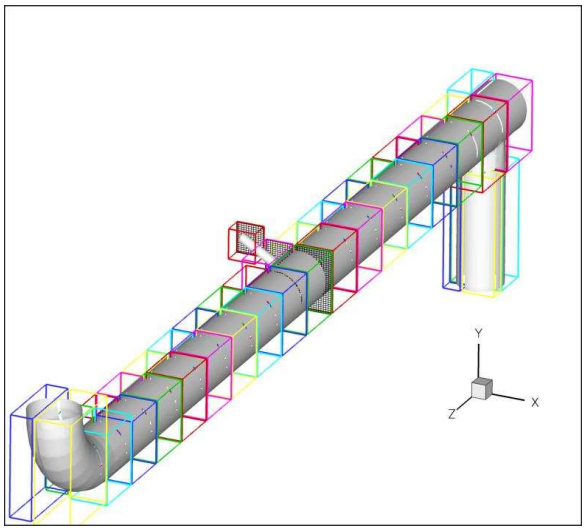

Figure 12: Computational multi-block domain and grid using IST/BMR.

Emergency Core Cooling (ECC) injection of cold water is one of the most severe scenarios of the global Pressurized Thermal Shock (PTS), referring to the occurrence of thermal loads on the Reactor Pressure Vessel (RPV), under pressurized conditions (Lucas et al., 2008). Here cold water is injected into the cold leg during a hypothetical Small Break Loss Of Coolant Accident (SB-LOCA). The injected water mixes with the hot fluid present in the cold leg and the mixture flows towards the downcomer where further mixing with the ambient fluid takes place. Very steep thermal gradients may damage the structural components while the primary circuit pressurisation is partially preserved. Therefore, the transient fluid temperature must be reliably assessed to predict the loads upon the RPV and the pressure wall toughness. The coolant can be single- or two-phase flow, depending on the leak size, its location and the NPP operating conditions. The PTS has been the objective of a number of international cooperative programs in the past, e.g. the OECD-ICAS as given by Sievers et al. (2000).

The computation of this severe scenario is now within reach of the averaged two-fluid formulation. Yao et al. (2005) solved for the purpose the 3D steady-state Navier-Stokes equations within the two-fluid framework (accounting for condensation, too), using a modified turbulent K-E model that accounts for the production by interfacial friction. The CATHARE code was then used; though recent attempts by the same group using the NEPTUNE-CFD code developed within the NURESIM EU project have been reported in several conferences. The time-averaged velocity profiles are somewhat well predicted, but not the turbulent quantities, in particular the turbulent kinetic energy and the shear-stress distributions. The question here is whether the latest transition in computational thermal-

hydraulics mentioned before relying on interface tracking than two-fluid modelling and LES or V-LES instead of RANS is feasible in this complex context or not. This is the reason why the test case presented here has was selected – as 'feasibility study'- towards more detailed simulation using the LEIS concept. The flow features more physics to deal with than the pipe flow for instance: two-phase flow, heat transfer, phase change, in a complex geometry with two inflows.

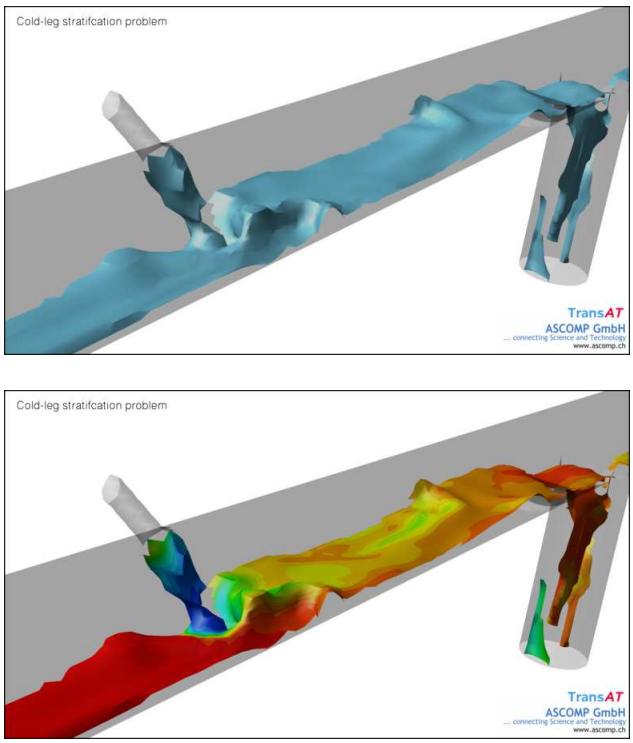

Figure 13: surface deformations at the injection and temperature contours

The flow conditions selected here for the simulation are taken from the D2.1.2 deliverable for the NRESIM EU project (Lucas and Bestion, 2007). More specifically, the pressure of the system is set to 20 bar, the water mass flow rate to 0.58 Kg/s, the steam flow rate to 0.2 Kg/s. The coolant fluid and the water in the leg are initially at temperature 296 K, the steam is fixed at saturation temperature: 485 K. Here we have again resorted to the MILES approach because the Reynolds number is again not very high, within the level set context. The level set equation (4) was modified to account for direct phase change, without modelling; the rate of mass transfer is rather directly inferred from the balance of energy fluxes across the interface. The grid was generated using the IST method described in Section 3 above, whereby a CAD file of the piping systems was embedded within a Cartesian grid; the geometry included the wire. The diameter of the pipe is 118 mm, the length is 1400 mm, the diameter of the IS port is 21.9 mm, with an inclination of 30 deg. The BMR technique for multi-block refinement was used, as shown in Figure 12. The grid was overall rather coarse, consisting at the end of 520.000 cells. The cross section was covered by 20x20 grids, which is rather coarse, but that does not mean that the resolution does not prevent capturing most of the flow details. This is obviously coarse, set for the sole purpose of feasibility study of the approach. An initial perturbation of the flow based on the shear Reynolds number was set in the leg.

Qualitative flow features are depicted in Figure 13, showing the interface deformations subsequent to coolant-jet impingement on the surface of the hot water in the leg, together with the temperature field as it mix downstream. The deformations of the sheared surface are most intense in the region below injection; the subsequent waves that form travel in the flow direction up to the wire level.

Figure 14 depicts several cross-flow planes inside the leg, showing secondary velocity vectors, interface level and temperature contours. The images start from left to right with flow direction: the first four panels depict the flow prior to injection; the fifth one depicts the flow at injection level; the 8th panel depicts the flow at the wire. The first panel shows heated water in the leg subsequent to steam injection at the inflow; the steam penetrates there quite deep and thus rising the temperature of the water to almost the steam temperature. The temperature of the steam does not remain constant at saturation conditions because the steam releases heat to the pipe walls, the temperature of which was set constant (296 K), too (isothermal boundary conditions).

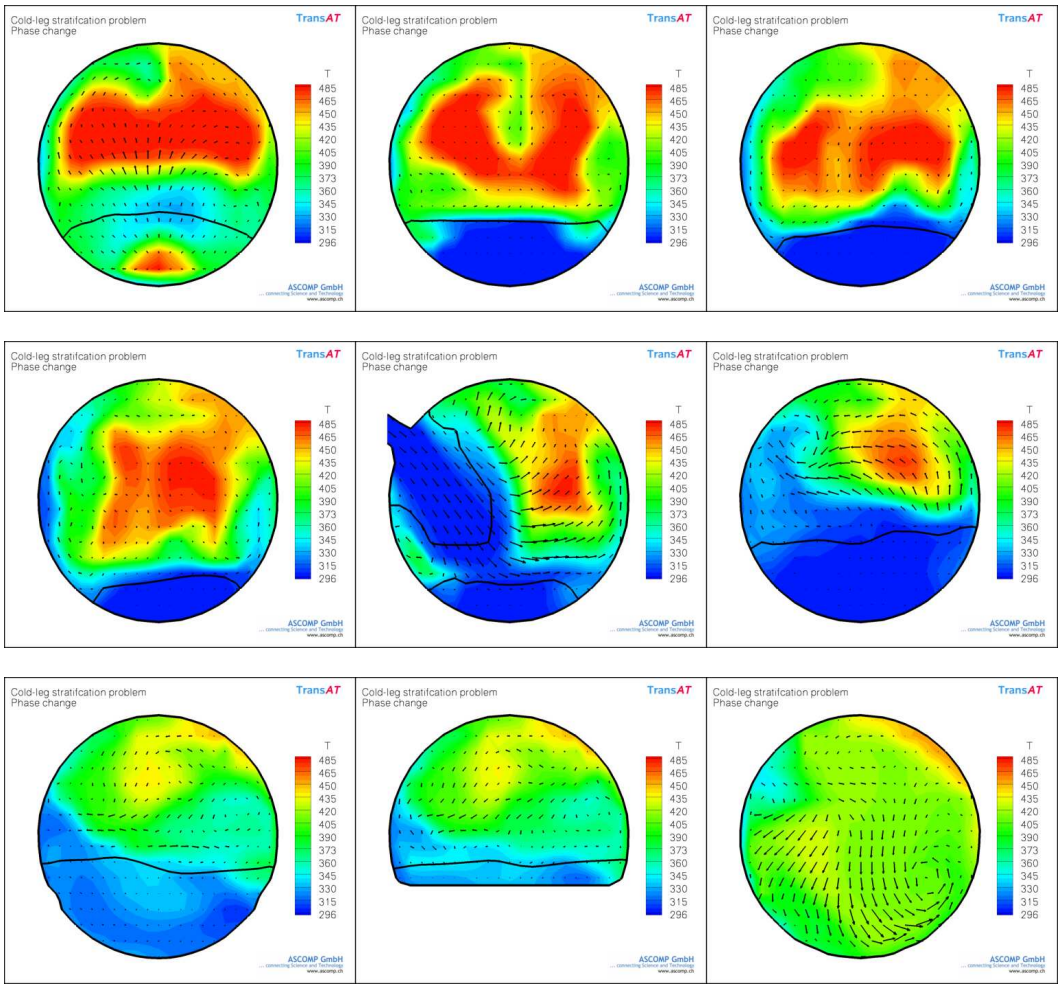

Figure 14: Positive and negative vorticity contours (x and z components)

The picture would have substantially changed if indeed adiabatic boundary conditions were set at the wall pipe surfaces. The heat is shown to diffuse from the steam to the water in the core leg rather gradually, in contrast to the case if saturation conditions of the steam were forced by neglecting the heat transfer flux, keeping only that in the liquid. The 7th panel shows that just before the wire the water temperature mixes well with the steam and reaches levels of 350 K.

7. CONCLUDING REMARKS AND FUTURE DEVELOPMENTS

The paper aimed at describing the way computational thermal-hydraulics is migrating to more sophisticated modelling techniques, transcending the two-fluid formulation and steady-state RANS equations for turbulence by integrating ITM's within the LES framework, defined here as "LEIS". The case studies outlined in this paper illustrate what can be done with LEIS for a class of turbulent

interfacial two-phase flows. The method can be successfully combined to generate realistic transient simulations of turbulent interfacial flows in reasonable computing times (of the order of 24H on PC Linux clusters). The perspectives for extension and generalization of such strategies to a variety of thermal-hydraulics problems are real, in view of the ever-increasing computational resources. However, we are still far from the computational power needed to fully simulate with this method more complex situations like a bubbly plume.

The LEIS has the great merit to avoid having to postulate various closure laws and models for interfacial friction, drag and lift forces, large-scale turbulence, interface induced production of turbulence, interfacial heat and mass transfer, etc. Still, the approach still requires fine tuning as to interface-turbulence interactions, which are not fully understood from the physical stand point, and thus not yet amenable to modelling. Flows featuring strong topology changes leading to interface break-up, for example, will need to be approached differently: sub-grid IS motions like droplets or bubbles (atomization) smaller than the grid should be tracked individually using the Lagrangian approach. Flows featuring both heavily mixed phases and interfacial two-phase flows in some portions will need to dynamically couple the two-fluid with ITM's. Another route to better resolve interfacial layers is the Adaptive Mesh Refinement technique (AMR) around evolving interfaces.

Acknowledgements

The theoretical part of the work mentioned here was initiated at ETH-Zurich under the supervision of Prof. George Yadigaroglu, more precisely at the CMFD group (Dr P. Liovic, Dr M. Fulgosi, Dr C. Narayanan, Dr S. Reboux). The new simulations shown here were conducted using the TransAT code of ASCOMP by Daniel Caviezel and "Chidu" Narayanan, partially within the NURESIM project.

REFERENCES

R. Collins. D.E Moraes, J. F. Davisdson, and D. Harrison, "The motion of a large gas bubble rising through liquid flowing in a tube," J. Fluid Mech., 89, 3, 497-514, 1978.

M. Fulgosi, D. Lakehal, S. Banerjee, and V. De Angelis, "Direct Numerical Simulation of Turbulence in a Sheared Air-Water Flow with a Deformable Interface," J. Fluid Mech., 482, 319-345, 2003.

C. Fureby, F.F. Grienstein, "Monotonically Integrated LES of free shear flows", AIAA Journal, 37, 544-556, 1999.

M. Germano, U. Piomelli, P. Moin, W. H. Cabot, "A Dynamic Sub-grid-Scale Eddy Viscosity Model," Phys. Fluids, 3, 1760-1765, 1991.

C.W. Hirt, B.D. Nichols, "Volume of fluid (VOF) method for the dynamics of free boundaries", J. Comp. Phys. 39, 201-219, 1981.

T. Hughes, A. Oberai, L. Mazzei, "LES of turbulent channel flows by the variational multiscale method," Phys. Fluids, 13, 1784, 2001.

D. Jamet, O. Lebaigue, N. Coutris, J.M. Delhaye, "The Second Gradient Method for the DNS of Liquid-Vapor Flows with Phase Change," J. Comp. Physics, 169, 624-651, 2001.

I. Kataoka, "Local Instant Formulation of Two-Phase Flow," Int. J. Multiphase Flow, 12, 745 (1986).

E. Labourasse, D. Lacanette, A. Toutant, P. Lubin, S. Vincent, O. Lebaigue, J-P. Caltagirone, P. Sagaut, "Towards large eddy simulation of isothermal two-phase flows: Governing equations and a priori tests", J. Multiphase Flow, 33, pp: 1-39, 2007.

D. Lakehal, “On the Modelling of Multiphase Turbulent Flows for Environmental & Hydrodynamics Applications”, Int. J. Multiphase Flow, 28(5), 823-857, 2002.

D. Lakehal, M. Meier, and M. Fulgosi, “Interface Tracking towards the Direct Simulation of Heat and Mass Transfer in Multiphase Flows,” Int. J. Heat & Fluid Flow, 23, 242-257, 2002a.

D. Lakehal, B. Smith, M. Milelli, “Large-eddy simulation of bubbly turbulent shear flows”. Journal of Turbulence, 3(25), 1-21, 2002b.

D. Lakehal, S. Reboux, P. Liovic, “SGS turbulence modelling for the LES of interfacial gas-liquid flows”, La Houille Blanche - Revue Internationale de l'Eau, 6, 125-131, 2005.

H. Lemonnier, D. Jamet, O. Lebaigue, “Validation of advanced computational methods for multiphase flow”, Beguell House, New York, 2005.

P. Liovic, D. Lakehal and J-L. Liow, “LES of turbulent bubble formation and break-up based on interface tracking,” Direct and Large-Eddy Simulation - V, ERCOFTAC Series 9, B.J. Geurts, R. Friedrich, O. Métais (Eds.), Kluwer Academic Publishers, Dordrecht, 261-271, 2003.

P. Liovic, M. Rudman, J.L. Liow, D. Lakehal, D. Kothe, “A three-dimensional unsplit-advection volume tracking with planarity-preserving interface reconstruction”, Computers & Fluids, 35(9), 1011–1032, 2006.

P. Liovic, D. Lakehal, “Interface-turbulence interactions in large-scale bubbling processes”, Int. J. Heat & Fluid Flow, 28, 127-144, 2007a.

P. Liovic, D. Lakehal, “Multi-Physics Treatment in the Vicinity of Arbitrarily Deformable Fluid-Fluid Interfaces”, J. Comp. Physics, 222, 504-535, 2007b.

D. Lucas, D. Bestion, “Deliverable: Review of the Existing Data Basis for the Validation of Model for PTS", 6th Euratom Framework Program NURESIM, Deliverable D2.1.2, (2007), Sub-Project 2.

D. Lucas et al., “An overview of the Pressurized Thermal Shock issue in the context of the NURESIM project”, Science and Technology of Nuclear Installations, Special Issue on Computational Fluid Dynamics for Gas-Liquid Flows, available on line, (doi:10.1155/2009/583259), 1-13, 2008.
.
S. K. Misra, J. T. Kirby, M. Brocchini, F. Veron, M. Thomas, C. Kambhamettu, “The mean and turbulent flow structure of a weak hydraulic jump”, Phys. Fluids, 20, 035106, 2008.

S. Martin, “Stratified flow instability and slug formation with condensation in a horizontal refrigerant pipe”, Proc. NURETH-11, Avignon, 2005.

S. Reboux, P. Sagaut, D. Lakehal, “Large-Eddy Simulation of Sheared Interfacial Two-Fluid Flow”, Phys. Fluids, 18 (10), 105105, 2006.

M. Sadatomi, A. Kawahara, K. Kano, S. Tanoue, “Flow characteristics in hydraulically equilibrium two-phase flows in a vertical 2-3 rod bundle channel”, J. Multiphase Flow, 30, 1093–1119, 2004.

J. Sievers *et al.*, “Thermal-hydraulic Aspects of the International Comparative Assessment Study on Reactor Pressure Vessel under PTS loading (RPV PTS ICAS)”, OECD/CSNI Workshop on Advanced Thermal-Hydraulic and Neutronic Codes: Current and Future Applications, Barcelona, 2000.

C. Speziale, “Computing non-equilibrium turbulent flows with time-dependent RANS and VLES”, Lecture Notes in Physics, Springer Berlin/Heidelberg, 490, 123-129, 1997.

S. Sussman, P. Smereka, S. Osher, “A Level set Approach for computing incompressible two-phase flow”, J. Comp. Physics, 114, 146-161, 1994.

S.O. Unverdi, G. Tryggvason, “A front-tracking method for viscous, incompressible, multi-fluid flows”, J. Comput. Phys. 100, 25-42, 1992

G. Yadigaroglu, D. Lakehal, “New trends in computational thermal hydraulics”, Nuclear Technology, 152 (2), 239-251, 2005.

W. Yao, D. Bestion, P. Coste, M. Boucker, “A three-dimensional two-fluid modeling of stratified flow with condensation for pressurized thermal shock investigations”, Nuclear Technology, 152(1), 129–142, 2005.